Evaluation of Snow Albedo in Land Models for Weather and Climate Studies

ZHUO WANG AND XUBIN ZENG

Department of Atmospheric Sciences, The University of Arizona, Tucson, Arizona

(Manuscript received 6 October 2008, in final form 11 August 2009)

ABSTRACT

Snow albedo plays an important role in land models for weather, climate, and hydrometeorological studies, but its treatment in various land models still contains significant deficiencies. Complementary to previous studies that evaluated the snow albedo as part of an overall land model study, the snow albedo formulations as used in four major weather forecasting and climate models [European Centre for Medium-Range Weather Forecasts (ECMWF), National Centers for Environmental Prediction (NCEP) ''Noah'' land model, National Center for Atmospheric Research (NCAR) Community Land Model (CLM3), and NCEP global model] were directly evaluated here using multiyear Boreal Ecosystem–Atmosphere Study (BOREAS) in situ data over grass and forest sites. First, four idealized cases over grass and forest sites were designed to understand better the different albedo formulations in these models. Then the BOREAS data were used to evaluate snow albedo and relevant formulations and to identify deficiencies of each model. Based on these analyses, suggestions that involve only minor changes in parameters or formulations were made to significantly reduce these deficiencies of each model. For the ECMWF land model, using the square root of snow water equivalent (SWE), rather than SWE itself, in the computation of snow fraction would significantly reduce the underestimation of albedo over grass. For the NCEP Noah land model, reducing (increasing) the critical SWE for full snow cover over short (tall) vegetation would reduce the underestimate (overestimate) of snow albedo over the grass (forest) site. For the NCAR CLM3, revising the coefficient used in the ground snow-fraction computation would substantially reduce the albedo underestimation over grass. For the albedo formulations in the NCEP global model, replacing the globally constant fresh snow albedo by the vegetation-type-dependent Moderate-Resolution Imaging Spectroradiometer (MODIS) maximum snow albedo would significantly improve the overestimation of model albedo over forest.

1. Introduction

Albedo plays an important role in land surface energy balance, and it is strongly affected by snow cover. When trees (with a relatively low surface albedo) are present, they can extend above the snowpack, ''masking out'' the relatively high albedo of snow under canopy. This would lead to warmer winter temperatures than if trees were not present (e.g., Bonan et al. 1992). The snow albedo feedback is one of the recognized positive feedbacks in the climate system (e.g., Qu and Hall 2006): increased air temperature would reduce snow cover over the Northern Hemisphere extratropics, leading to less reflection of solar radiation, which would result in more warming because of the additional absorbed solar radiation.

The principles of snow albedo at a small spatial scale have been well established, with the spectral dependence, grain size and type, and contamination being important factors in the snow albedo computation (e.g., Wiscombe and Warren 1980; Warren and Wiscombe 1980). Marshall and Warren (1987) found that the spectrally averaged snow albedo varies with snow grain size, solar zenith angle (SZA), snow cover thickness, underlying surface albedo (for thin snow), and absorptive impurities in the snowpack. Among these factors, grain size is the most important variable controlling snow albedo: a photon has a chance of being scattered when it crosses an air–ice interface and has a chance of being absorbed only when it is passing through the ice; an increase in grain size causes an increase in the path length that must be traveled through the ice between scattering opportunities and hence reduces the snow albedo (Warren 1982). However, snow grain size is difficult to predict and is crudely parameterized in terms of the snow age and its temperature history (e.g., Anderson 1976).

Corresponding author address: Zhuo Wang, 1118 East 4th St., P.O. Box 210081, Department of Atmospheric Sciences, The University of Arizona, Tucson, AZ 85721.
E-mail: zhuowang@atmo.arizona.edu

DOI: 10.1175/2009JAMC2134.1

Snow albedo has been evaluated as part of an overall land model albedo study (Slater et al. 2001; Zhou et al. 2003; Oleson et al. 2003; Wang et al. 2004; Tian et al. 2004). For instance, Zhou et al. (2003) found that, relative to the Moderate-Resolution Imaging Spectroradiometer (MODIS) data, the Community Land Model (CLM) underestimates albedos in the visible band (0.3–0.7 μm) over northern high latitudes, mainly because of its overestimation of leaf area index (LAI) and stem area index (SAI), but overestimates albedos in the near-infrared band (0.7–5.0 μm) over Greenland and northern Canada. Their analysis indicates that CLM should better represent LAI, SAI, and vegetation albedo in the presence of snow. Snow albedo has also been evaluated as part of the snow submodel evaluation (Slater et al. 2001). For instance, the basic variables, including snow depth, snow albedo, snow water equivalent (SWE), snow cover fraction, and snow temperature, in the snow submodel of the Biosphere–Atmosphere Transfer Scheme (BATS) were evaluated using the available data in Yang et al. (1997). They found that the original snow cover parameterization underestimates snow cover fraction and surface albedo. Their suggested snow cover parameterization can correct this deficiency but also slightly degrades the simulated surface temperature and SWE.

However, because of nonlinear interactions between snow and other processes in land models, it is difficult from these studies to address questions such as, Is the snow albedo treatment itself in land models appropriate? For instance, a land model could have an earlier snowmelt for a variety of reasons, and the subsequent albedo in the model would be very different from the observed snow albedo. A typical land modeling study could easily claim that the simulated albedo is deficient; however, this bad model performance does not necessarily imply that the snow albedo formulation itself is incorrect. The purpose of this study is to address the above question by directly testing the snow albedo formulations as used in some of the major weather forecasting and climate research centers, including the National Centers for Environmental Prediction (NCEP)–Oregon State University–U.S. Air Force–National Weather Service Office of Hydrologic Development (Noah) land model (Mitchell et al. 2004) as used in regional and global weather forecasting at NCEP and in the Weather Research and Forecasting Model (WRF), the formulations used in the radiative transfer computation (Hou et al. 2002) of the NCEP Climate Data Assimilation System (denoted as NG in this paper), the land model used by the European Centre for Medium-Range Weather Forecasts (ECMWF; see http://www.ecmwf.int), and version 3 of the Community Land Model (CLM3; Oleson et al. 2004) in the Community Climate System Model at the National Center for Atmospheric Research (NCAR). Note that while Noah is the land component in the NCEP global models, the albedo computation is based on Hou et al. (2002; version denoted as NG). This work is complementary to previous studies (Boone and Etchevers 2001; Slater et al. 2001; Niu and Yang 2007) by focusing on process studies rather than running the land models with full physics. Note that more-sophisticated snow models have also been developed (e.g., Jordan 1991), but their use in weather and climate models has been limited because of their complexity and relatively higher computational cost. Therefore, these snow models are not included in this study.

The snow albedo treatments in the above four major models are briefly summarized in section 2. The four idealized cases are described in section 3, and the evaluation of snow formulations using in situ data is shown in section 4. The sensitivity tests are discussed in section 5, and a summary is given in section 6.

2. Snow albedo treatments in ECMWF, Noah, NG, and CLM3

a. ECMWF land model

In the ECMWF land model (http://www.ecmwf.int/research/ifsdocs/CY28r1), a land grid box is composed of three basic surface types: low vegetation, high vegetation, and bare ground. The low vegetation type with a fractional area of A_L is further divided into a vegetation portion with its fractional area $c_L = 0.85A_L$ and a bare-ground portion ($0.15A_L$). Likewise, the high vegetation type with a fractional area of A_H is divided into a vegetated portion ($c_H = 0.9A_H$) and a bare-ground portion ($0.1A_H$). The fractional area of total bare ground is $c_B = 1 - c_H - c_L$.

Here c_H is used to calculate the fractional area of snow overlying low vegetation and bare ground (c_5) and overlying high vegetation (c_7) as $c_5 = c_{\rm sn}(1 - c_H)$ and $c_7 = c_{\rm sn}c_H$, respectively. In these expressions, $c_{\rm sn} = \min(1, W/W_{\rm cr})$, W is the SWE (in meters), and $W_{\rm cr} = 0.015$ m is the minimum SWE that ensures complete coverage of the grid box.

Snow albedo for snow on low vegetation and bare ground ranges from 0.5 for old snow to 0.85 for fresh snow (Douville et al. 1995). To be specific, for nonmelting conditions, the decrease of snow albedo with time is computed as

$$\alpha_{\rm sn}^{t+1} = \alpha_{\rm sn}^{t} - \tau_a \Delta/86\,400, \tag{1}$$

where τ_a is the linear coefficient to decrease the albedo by 0.1 in 12.5 days ($\tau_a = 0.008$) and Δt is the time step (in seconds). For melting conditions,

$$\alpha_{\text{sn}}^{t+1} = (\alpha_{\text{sn}}^{t} - \alpha_{\text{min}}) \exp\left(\frac{-0.24\Delta t}{86\,400}\right) + \alpha_{\text{min}}, \qquad (2)$$

where $\alpha_{\text{min}} = 0.5$. If snowfall is higher than 1 kg m^{-2} h^{-1}, the snow albedo is reset to the maximum value $\alpha_{\text{sn}}^{t+1} = \alpha_{\text{max}} = 0.85$.

The albedo for high vegetation with snow underneath is fixed at 0.15 in the ECMWF land model. Observations suggest that, by and large, the albedo changes from a value that is around 0.3 just after a heavy snowfall to a value that is around 0.2 after a few days over areas with different types of forests (Betts and Ball 1997; Viterbo and Betts 1999). This change reflects the disappearance of intercepted snow as a result of melt for sufficiently warm temperature or wind drift for cold temperature. Ways of describing these two mechanisms would involve a separate albedo variable for either the snow in the presence of high vegetation or the intercepted snow by canopy. In the absence of either of the two, $\alpha_{\text{sn},f} = 0.15$ is used in the ECMWF model for snow in the presence of high vegetation based on Viterbo and Betts (1999).

b. Noah land model

The Noah land surface model (Mitchell et al. 2004) provides the land component for the regional and global weather forecasting models at NCEP and for the version of the WRF at NCAR. The treatment of snow and frozen ground in Noah is described in Koren et al. (1999).

The fractional snow coverage is computed as a function of SWE (W):

$$f_{\text{sn}} = 1 - \exp\left(-\alpha_s \frac{W}{W_{\text{cr}}}\right) + \frac{W}{W_{\text{cr}}} \exp(-\alpha_s), \qquad (3)$$

where α_s is a distribution shape parameter and W_{cr} is the threshold SWE above which f_{sn} is 100%. Equation (3) fits the empirical areal snow depletion curves from Anderson (1973) well for α_s varying from 2 to 4 (Koren et al. 1999). In Noah, $\alpha_s = 2.6$, $W_{\text{cr}} = 0.04$ m for grass, and $W_{\text{cr}} = 0.08$ m for forest.

The albedo including snow effect is then computed as

$$\alpha = \alpha_{\text{sn-free}} + f_{\text{sn}}(\alpha_{\text{sn,max}} - \alpha_{\text{sn-free}}), \qquad (4)$$

where $\alpha_{\text{sn-free}}$ is the snow-free albedo and $\alpha_{\text{sn,max}}$ is the maximum albedo over deep snow. Maximum snow albedo $\alpha_{\text{sn,max}}$ and monthly $\alpha_{\text{sn-free}}$ values are specified for each grid cell based on satellite data at NCEP (Robinson and Kukla 1985). In contrast, $\alpha_{\text{sn-free}}$ and $\alpha_{\text{sn,max}}$ are prescribed for each vegetation type for the NCAR version of WRF (Chen and Dudhia 2001).

c. NCEP global model (NG)

Whereas Noah is the land component in the regional and global models at NCEP and in the version of WRF at NCAR, a different albedo treatment (Hou et al. 2002) is still used operationally at NCEP in its global modeling systems (the medium-range Global Forecast System, the ocean–atmosphere coupled Climate Forecast System, and the Climate Data Assimilation System). In this albedo scheme, Hou et al. (2002) used a seasonally varying surface albedo dataset at 1° horizontal resolution developed based on Briegleb (1992) and Briegleb et al. (1986). Each seasonal albedo dataset contains background surface diffuse albedo for a strong or weak SZA dependency in the visible (VIS; $\lambda \leq 0.7$ μm) and near-infrared (NIR; $\lambda \geq 0.7$ μm) bands (denoted as $\alpha_{S,\text{VIS}}$, $\alpha_{W,\text{VIS}}$, $\alpha_{S,\text{NIR}}$, and $\alpha_{W,\text{NIR}}$, respectively), as well as the fractional coverage of the surface vegetation types with strong or weak zenith angle dependence (i.e., f_S or f_W). The area-weighted averages α_{dif} are used to represent the snow-free diffuse albedos (e.g., $\alpha_{S,\text{VIS}} f_S + \alpha_{W,\text{VIS}} f_W$ for the average diffuse albedo in the VIS band). The snow-free direct albedo α_{dir} is then computed from

$$\alpha_{\text{dir}}(\theta) = \alpha_{\text{dif}} \frac{1 + C}{1 + 2C\cos\theta}, \qquad (5)$$

where α_{dif} is the seasonal diffuse albedo discussed above and θ is the SZA. Of the 13 vegetation types used in Hou et al. (2002), seven types are characterized by a strong SZA dependence with $C = 0.4$ in Eq. (5) and the remaining types are characterized by a weak SZA dependence with $C = 0.1$.

In a given land grid, the fraction of snow-covered area is computed from

$$f_{\text{sn}} = \frac{20W}{z_0 + 20W} f_H, \qquad (6)$$

where W is SWE, z_0 is the roughness length for momentum (about 10% of vegetation height), and f_H is a shading factor related to the subgrid variation of orography and is limited to be between 0.2 (for rugged mountainous orography with high variances) and 1 (for flat terrain). In this study, f_H is not considered and is assumed to be 1.

The diffuse snow albedo $\alpha_{\text{sn}}^{\text{diff}}$ is prescribed as 0.9 and 0.75 for the VIS and NIR bands, respectively. The direct snow albedo is taken to be the same as the diffuse albedo for SZA lower than 60°, whereas it is dependent on SZA for SZA higher than 60° based on Briegleb (1992):

$$\alpha_{\mathrm{sn}}^{\mathrm{dir}}(\theta) = \alpha_{\mathrm{sn}}^{\mathrm{dif}} + 0.5(1 - \alpha_{\mathrm{sn}}^{\mathrm{dif}})\left(\frac{3}{1 + 4\cos\theta} - 1\right). \quad (7)$$

The four components (direct and diffuse albedos for the VIS and NIR bands) of total surface albedo are obtained as the area-weighted averages of snow-free and snow albedos.

d. NCAR CLM3

The NCAR CLM3 (Oleson et al. 2004) separately computes albedos for soil, snow, and vegetation and then takes the total albedo of a grid box as an average of these albedos weighted by the representative area fractions. These albedos are computed based on the two-stream scheme for radiative transfer in plant canopies (Dickinson 1983; Sellers 1985; Bonan 1996) under three assumptions: 1) fluxes are isotropic in the upward and downward directions only, 2) the canopy is horizontally uniform, and 3) the scattering and absorbing elements in the canopy are randomly distributed in space. Under these assumptions, the direct and diffuse albedos are obtained from the complicated analytical solutions of the radiative transfer equations that are related to the following factors: the scattering coefficient, upscatter parameters for diffuse and direct beam radiation, the optical depth of direct beam per unit leaf and stem area, solar zenith angle, and the average inverse diffuse optical depth per unit leaf and stem area.

The ground snow fraction f_{sno} is computed from

$$f_{\mathrm{sno}} = \frac{z_{\mathrm{sn}}}{10 z_{0m,g} + z_{\mathrm{sn}}}, \quad (8)$$

where z_{sn} is the snow depth (m) and $z_{0m,g} = 0.01$ m is the momentum roughness length for soil. Then the ground albedo is taken as the area-weighted average of snow-free and snow albedos. The snow-free soil albedo depends on the prescribed soil color and soil moisture (Dickinson et al. 1993).

The snow albedo α_{sn} depends on SZA and snow age. For SZA lower than 60°, the direct beam snow albedo $\alpha_{\mathrm{sn}}(\theta)$ is the same as the diffuse snow albedo (taken as 0.95 and 0.65 for VIS and NIR, respectively). For SZA higher than 60°, the SZA dependence is considered to be

$$\alpha_{\mathrm{sn,VIS}}(\theta) = 0.95(1 - 0.2 f_{\mathrm{age}}) + 0.2[1 - 0.95(1 - 0.2 f_{\mathrm{age}})] \times \left(\frac{3}{1 + 4\cos\theta} - 1\right) \quad \text{and} \quad (9)$$

$$\alpha_{\mathrm{sn,NIR}}(\theta) = 0.65(1 - 0.5 f_{\mathrm{age}}) + 0.2[1 - 0.65(1 - 0.5 f_{\mathrm{age}})] \times \left(\frac{3}{1 + 4\cos\theta} - 1\right), \quad (10)$$

where f_{age} is a transformed snow age used to give the fractional reduction of snow albedo resulting from snow aging effect:

$$f_{\mathrm{age}} = 1 - \frac{1}{1 + \tau_{\mathrm{sn}}}. \quad (11)$$

The nondimensional age of snow τ_{sn} is incremented as a model prognostic variable at each time step as follows:

$$\begin{aligned} \Delta\tau_{\mathrm{sn}} &= \tau_0(r_1 + r_2 + r_3)\Delta t \quad \text{for} \quad 0 < W \le 800 \\ &= 0 \qquad\qquad\qquad\quad \text{for} \quad W > 800, \end{aligned} \quad (12)$$

where Δt is the model time step (s), $\tau_0 = 1 \times 10^{-6}$ (s^{-1}), and W is the SWE (kg m^{-2}). The term r_1 represents the effect of grain growth due to vapor diffusion (and therefore surface temperature of the top snow layer), the term r_2 represents the additional effect near and at melting point (0°C), and the term r_3 represents the effect of dirt and soot [see Oleson et al. (2004) for more details].

In addition to ground snow cover, CLM3 considers the vegetation fraction covered by intercepted snow:

$$\begin{aligned} f_{\mathrm{wet}} &= \left[\frac{W_{\mathrm{can}}}{p(L+S)}\right]^{2/3} \le 1 \quad L + S > 0 \\ &= 0 \qquad\qquad\qquad\quad L + S = 0, \end{aligned} \quad (13)$$

where W_{can} is the SWE intercepted by canopy and $p(L + S)$ is the maximum amount of SWE the canopy can hold, where $(L + S)$ represents the leaf and stem area index and $p = 0.1$ mm. Note that Eq. (13) is also used in CLM3 for rainfall intercepted by canopy with W_{can} denoting the intercepted water. This fraction f_{wet} is used (e.g., by modifying the scattering coefficient) in the two-stream radiative transfer computation of surface albedo (Oleson et al. 2004).

Furthermore, CLM3 considers the vertical fraction of vegetation covered by snow as

$$f_{\mathrm{veg}}^{\mathrm{sn}} = \frac{z_{\mathrm{sn}} - z_{\mathrm{bot}}}{z_{\mathrm{top}} - z_{\mathrm{bot}}} \quad \text{for} \quad z_{\mathrm{sn}} - z_{\mathrm{bot}} \ge 0, \quad (14)$$

where z_{top} and z_{bot} are the heights of the canopy top and bottom, respectively. The leaf and stem area indices are then adjusted for vertical snow burial as

$$A = A^*(1 - f_{\mathrm{veg}}^{\mathrm{sn}}), \quad (15)$$

where A^* is the leaf or stem area before adjustment for snow and A is the remaining exposed leaf or stem area used in the two-stream radiative transfer computation in CLM3.

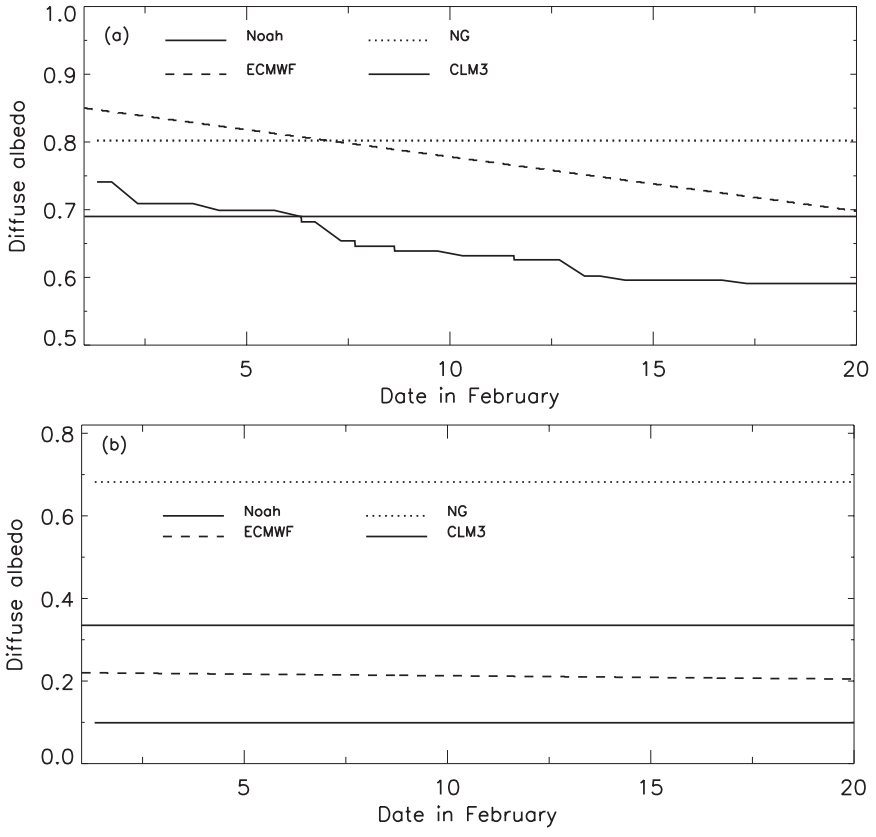

FIG. 1. Temporal variation of diffuse albedo (a) over the grass site (52.16°N, 106.6°W) and (b) over the forest site (53.92°N, 104.69°W) from 1 to 20 Feb for the idealized cases 1 and 2.

3. Four idealized cases

For simplicity, we compare snow age, snow fraction, direct albedo, and diffuse albedo among different models in four idealized cases without new snowfall or snowmelt at the Boreal Ecosystem–Atmosphere Study (BOREAS) grass site (52.16°N, 106.6°W) and the forest site (53.92°N, 104.69°W) over old jack pine.

a. Case 1 (low vegetation with deep snow)

Grass is assumed to be covered by snow of 1 m in depth (to ensure full snow cover) with 100 kg m^{-3} as the initial snow density at the BOREAS grass site. The model formulations were run for 20 days starting from 0000 local standard time (LST) 1 February.

In ECMWF, full vegetation cover ($A_L = 1$) is assumed, and the initial albedo is assumed to be the maximum snow albedo (0.85). Then Eq. (1) is used to compute the variation of albedo with time.

In Noah, SWE is constant (because there is no new snowfall or snowmelt in this idealized case) and can be obtained from the initial snow density and snow depth. Equations (3) and (4) are then used to compute the snow fraction and snow-covered surface albedo. The snow-free albedo $\alpha_{\text{sn-free}}$ is obtained from a lookup table, and maximum snow albedo $\alpha_{\text{sn,max}}$ is obtained from vegetation-type-dependent MODIS maximum snow albedo data (Barlage et al. 2005).

In NG, Eq. (6) with the orography factor $f_H = 1$ (flat-terrain assumption) is used to compute the snow fraction, and Eq. (7) is used to compute the snow albedo. The albedo for the grid cell is the average of snow-free albedo and snow albedo using snow fraction as the weighting factor.

In CLM3, full vegetation cover is assumed along with a leaf and stem area index (LSAI = LAI + SAI) of 0.5. The fraction of the ground covered with snow is computed from Eq. (8), and then LSAI is adjusted by Eq. (15). The direct snow albedos in the VIS and NIR bands are computed from Eqs. (9) and (10). The direct albedo in the shortwave band is obtained from the average of snow albedo in the VIS and NIR bands.

Since CLM3 and ECMWF consider the snow aging process, their albedos decrease with time (Fig. 1a). Because SWE is assumed to be constant for this idealized case, snow albedo in Noah and NG does not change with

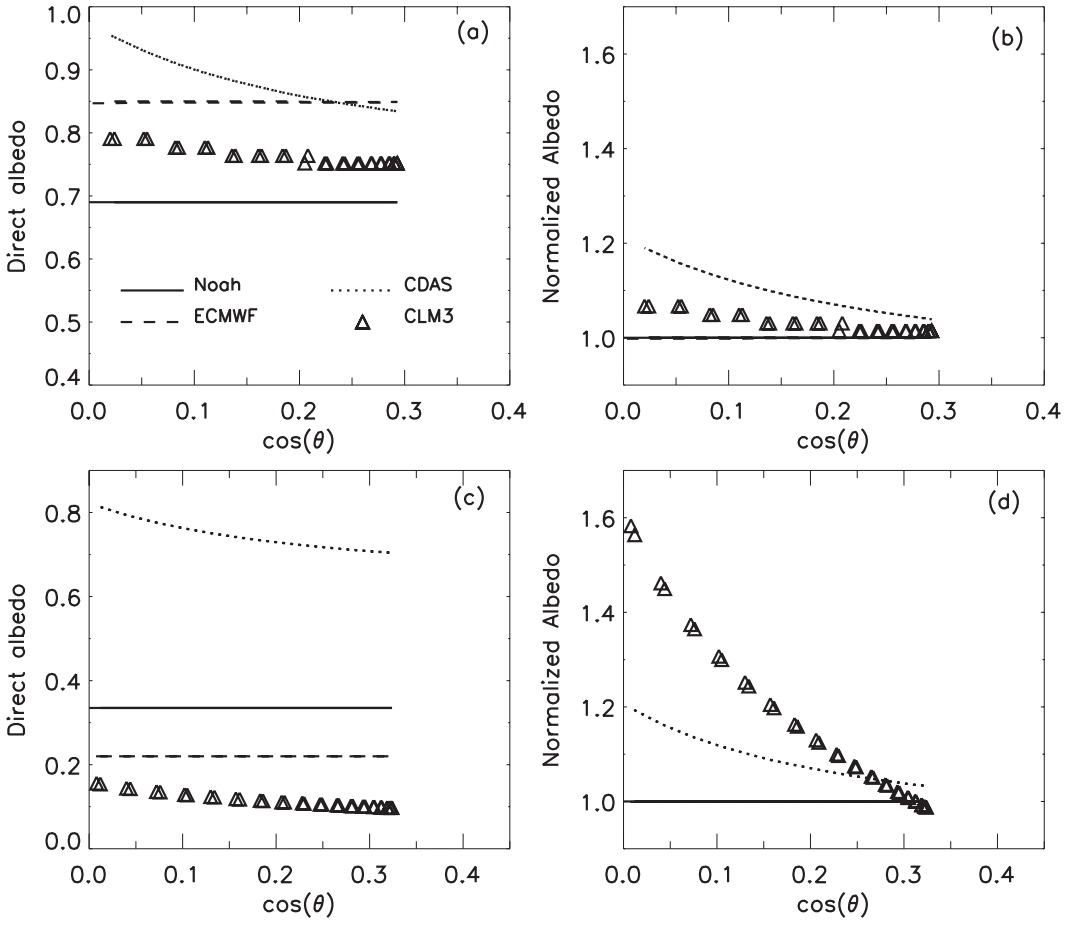

FIG. 2. Comparison of the (left) black-sky (or direct) albedo and (right) its normalized values by its corresponding diffuse albedo on 1 Feb (a),(b) over the grass site (52.16°N, 106.6°W) for the idealized case 1 and (c),(d) over the forest site (53.92°N, 104.69°W) for the idealized case 2.

time (Fig. 1a). For such an idealized case, the albedos at the beginning or end of the integration are still very different among the four models (Fig. 1a), suggesting that the measurement and land modeling communities need to work more closely to address this type of resolvable issues.

b. Case 2 (high vegetation with deep snow)

Case 2 is the same as case 1 but is for the BOREAS forest site with 2 m of snow on the ground (under trees). Vegetation cover $A_H = 1$ in ECMWF, and LSAI is taken as 4 in CLM3. The model formulations were run for 20 days, starting from 0000 LST 1 February.

Comparison of the diffuse albedos over the grass versus forest sites in Figs. 1a and 1b indicates that NG treats snow above grass and snow under trees in the same way in computing the snow fraction in Eq. (6). Because $f_{sn} = 1$ in Eq. (3) over these two sites in Noah, the significantly different albedos over the two sites reflect the use of different maximum snow albedos over these sites. The ECMWF snow albedo in Fig. 1b is slightly higher than the prescribed 0.15 for snow under trees, because fractional tree cover is assumed to be 0.9 and snow over the bare-ground fraction (0.1 of the grid cell) has a much higher albedo. With the explicit treatment of snow on the ground, snow burial fraction, and snow intercepted by canopy, CLM3 is able to distinguish snow above grass in Fig. 1a versus snow under trees in Fig. 1b.

As mentioned earlier, the SZA dependence is not considered in Noah or ECMWF, but it is considered in NG and CLM3. For example, Figs. 2a and 2b show the black-sky (or direct) albedo (BSA) and its normalized values on the first day of integration (1 February). Both BSA and normalized BSA increase with SZA faster in NG than in CLM3 over the grass site. If the aging factor f_{age} is not considered in CLM3 [i.e., in Eqs. (9) and (10)], the functional form of Eqs. (9) and (10) is the same as that in Eq. (7) for NG. However, the SZA-dependent factor (0.5) in NG is different from that (0.2) in CLM3,

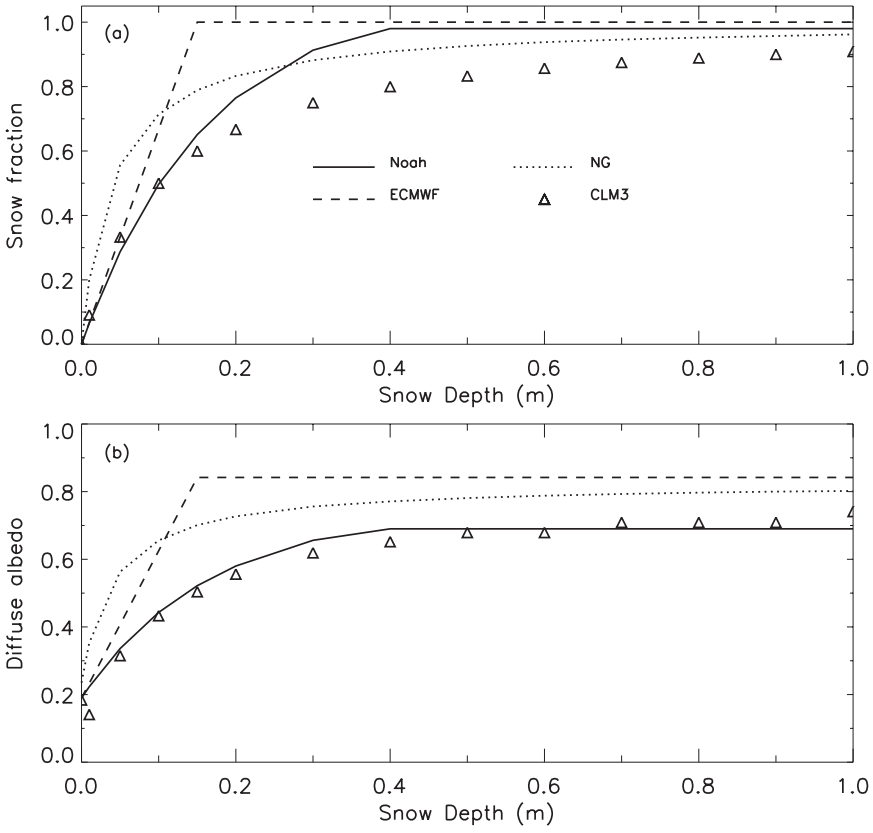

FIG. 3. Comparison of (a) snow cover fraction and (b) diffuse albedo as a function of snow depth for four land surface models over the grass site at local noon on 1 Feb for the idealized case 3.

which is the reason for their different albedo dependences on SZA in Figs. 2a and 2b. Note that whereas these formulations originally came from Dickinson et al. (1986), in which the factor of 0.2 was used, the value of 0.5 in Eq. (7) was adopted in Briegleb (1992) and used in Hou et al. (2002).

In NG, the albedo over the grass or forest site has the same SZA dependence in Eq. (7), as also shown in Figs. 2b and 2d. Through its two-stream radiative transfer computation, CLM3 shows a much stronger SZA dependence of the normalized albedo over the forest site (Fig. 2d) than over the grass site (Fig. 2b).

The snow cover fraction plays an important role in the computation of albedo and energy balance of the land surface (e.g., Cess et al. 1991). Therefore, cases 3 and 4 are designed to examine the snow cover fraction used in different models and its effect on snow albedo.

c. Case 3 (low vegetation with variable snow depth)

Case 3 is the same as case 1 (i.e., over the grass site) except for running the model formulations for one day with different initial snow depths from 0 to 1 m. Figure 3a shows that snow fraction based on Eq. (6) in NG (with grass roughness length $z_0 = 0.08$ m) initially increases fastest with snow depth but that ECMWF snow fraction reaches unity first at snow depth of 15 cm. In contrast, even with 1-m snow, the ground is still not fully covered in CLM3 or NG based on similar formulations [i.e., Eqs. (6) or (8)]. This problem has also been addressed in previous studies (e.g., Niu and Yang 2007). Note that snow fraction is capped at 0.98 in Noah.

d. Case 4 (high vegetation with variable snow depth)

Case 4 is the same as case 2 (i.e., over the forest site) except for running the model formulations for one day with different initial snow depths from 0 to 2 m. ECMWF snow fraction is independent of vegetation types (Figs. 3a and 4a). In strict terms, this fraction only refers to the snow fraction on the ground (under trees) and the shading effect is implicitly considered by prescribing a constant (0.15) albedo for snow under trees in ECMWF (Fig. 4b). In a similar way, the ground snow fraction in CLM3 is computed in Eq. (8), independent of vegetation types. Then the two-stream radiative transfer computation

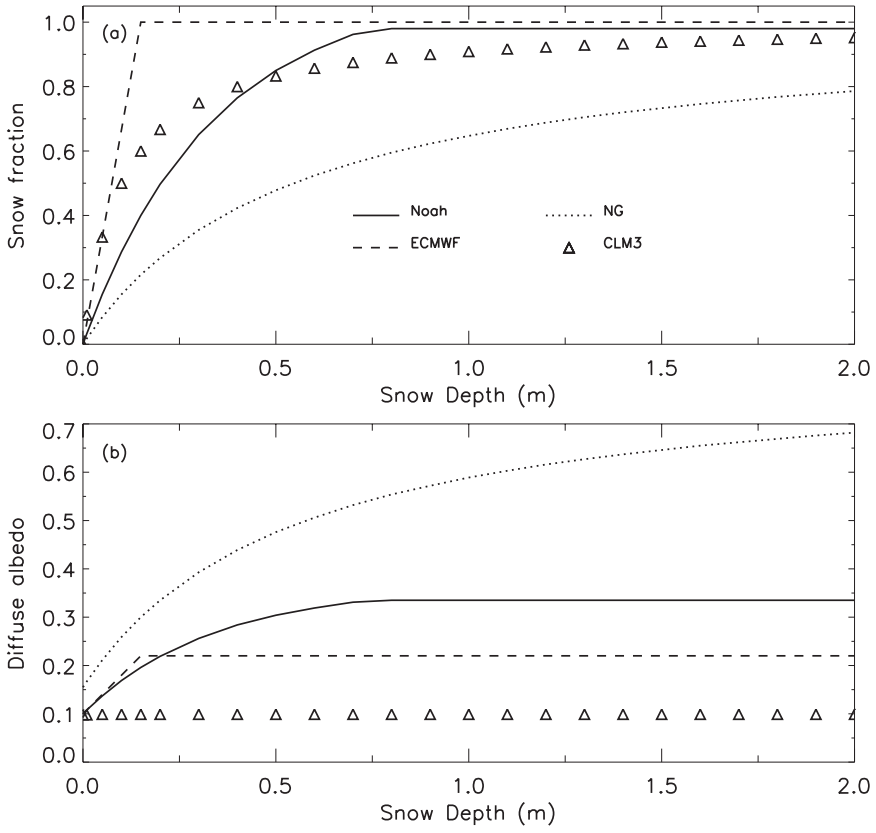

FIG. 4. As in Fig. 3, but over the forest site for the idealized case 4.

yields different albedos over the grass and forest sites (Figs. 3b and 4b). While the diffuse albedo over the forest site converges to a value that is significantly smaller than over the grass site in Noah, ECMWF, and CLM3 (which is qualitatively correct), it still increases with snow depth in NG even after snow depth is greater than 1 m, which is incorrect.

4. Comparison of model results with in situ data

The above four cases consider the idealized conditions but do not compare with the observational data. BOREAS was a large-scale, multidisciplinary project focusing on understanding how the boreal ecosystem would respond to a change in climate (Sellers et al. 1995). The BOREAS study region covered most of Saskatchewan and Manitoba in Canada, containing northern study areas and southern study areas within which process study sites were located (Sellers et al. 1997). A more detailed description of the site locations, site environments, and instruments can be found in Shewchuk (1997). Here the BOREAS in situ data from 1994 to 1996 over a grass site (52.16°N, 106.6°W) and a forest site (53.92°N, 104.69°W) (Betts and Ball 1997) are used. The same sites were also used in the above idealized case studies.

Because we intend to test model albedo formulations directly (without running the land model), we only select periods with snow on the ground but without snowfall or snowmelt for the model–data comparison. Figure 5a compares model albedos (including SZA dependence) with observations for 7 March 1996 when the above criteria were met. A single plant functional type (i.e., grass) is used for each model along with default model parameters for the month of March (e.g., leaf and stem area indices of 0.5 and 0.3, respectively, in CLM3). Because in situ measurements provide the blue-sky albedo only (i.e., the total albedo due to direct and diffuse radiations), we have also plotted the model blue-sky albedos as the average model black-sky (or direct) and white-sky (or diffuse) albedos weighted by the observed diffuse ratio. It is obvious that the SZA dependence of the blue-sky albedo is weaker than that of the black-sky albedo (e.g., Fig. 5a vs Fig. 2a; Wang and Zeng 2008). In comparison with observations, CLM3 and Noah significantly underestimate the albedo (Fig. 5a) because of relatively small snow fraction (Fig. 3a). NG albedo is closest to observations because it has the highest

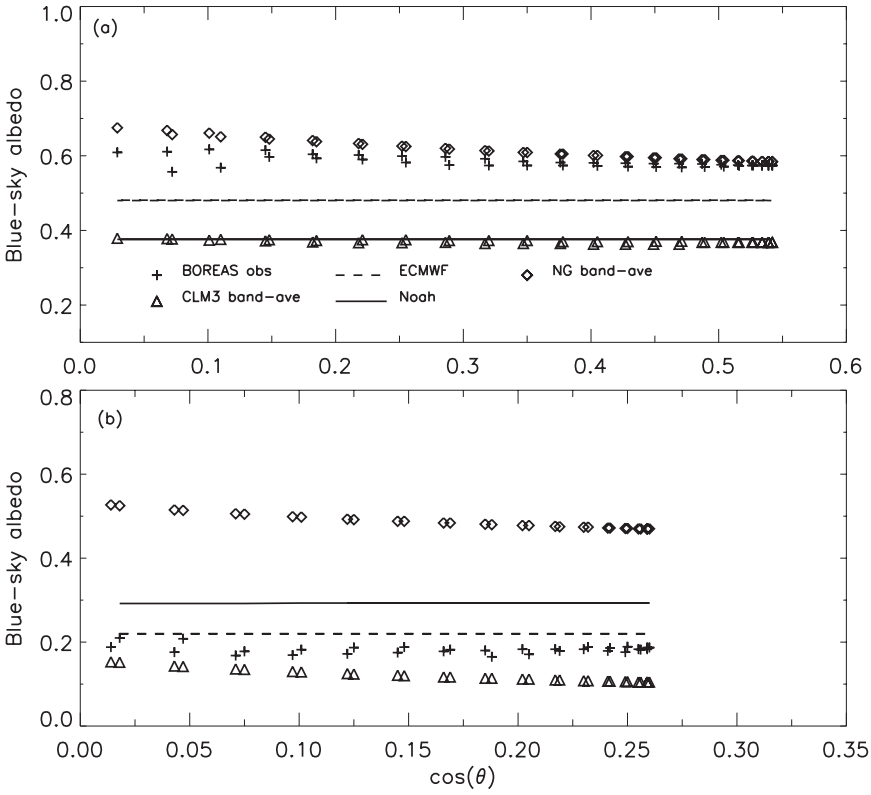

FIG. 5. Comparison of blue-sky albedos from the BOREAS measurements, CLM3, Noah, NG, and ECMWF (a) over the grass site on 7 Mar 1996 (with a snow depth of 0.072 m) and (b) over the forest site on 16 Jan 1996 (with a snow depth of 0.45 m). There was no snowfall or snowmelt in these days.

snow fraction among the four models for shallow snow (Fig. 3a).

Figure 5b shows the corresponding results over the BOREAS forest site on 16 January 1996 with snow depth of 0.45 m. ECMWF results are closest to observations because these observations were the basis for prescribing a constant albedo for snow under trees in the ECMWF land model (Viterbo and Betts 1999). CLM3 results are also reasonable because the two-stream approximation can partially handle the forest shading of underlying snow with the leaf and stem area indices of 2.8 and 0.6, respectively. Sensitivity tests will be done later to address the dependence of results on LAI and SAI in CLM3. Even though NG has the smallest snow fraction (Fig. 4a), it still has the highest snow albedo (Fig. 4b), which is much higher than the observed values (Fig. 5b). The reason is that NG does not consider the forest shading effect of underlying snow. Even though the snow fraction from Noah is 2 times that from NG for this case with 0.45-m snow (Fig. 4a), the Noah snow albedo is still smaller than that of NG (Figs. 4b and 5b) because of the use of maximum snow albedo that (at least partially) considers the forest shading effect of underlying snow. However, Noah snow albedo is still higher than the observations (Fig. 5b).

To address the robustness of the results in Fig. 5, we have also evaluated the multiyear BOREAS data (from 1994 to 1996) over the grass and forest sites to pick up days that meet the criteria used for Fig. 5; results are summarized in Fig. 6. Each point represents the daily-averaged blue-sky albedo for each of the days with snow on the ground but without snowfall or snowmelt. Over the grass site, CLM3, Noah, and, to a lesser degree, ECMWF underestimate the albedo (Fig. 6a), consistent with results in Fig. 5a. Although NG albedo is slightly higher than observed values for one day in Fig. 5a, it is overall smaller than the observed values when the complete BOREAS data are analyzed (Fig. 6a), indicating the importance of using long-term observations. Over the forest site, CLM3 and ECMWF albedos are relatively close to measurement but Noah and NG overestimate albedo (Fig. 6b), consistent with results from Fig. 5b.

Snow albedo is generally reduced because of the snow aging effect (i.e., increasing snow grain size and dirt and soot content). Among the above four models, CLM3 and ECMWF consider the snow aging process in albedo

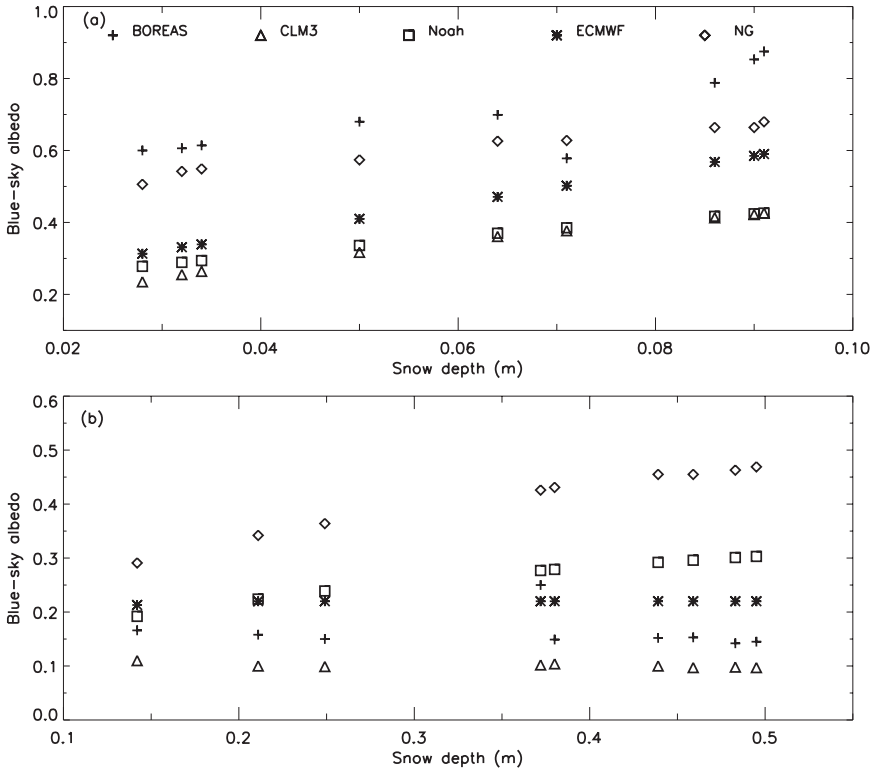

FIG. 6. Comparison of daily averaged blue-sky albedos from CLM3, Noah, NG, and ECMWF with the multiyear BOREAS data (from 1994 to 1996) on the days that meet the criteria used for Fig. 5 over the (a) grass and (b) forest sites.

computation; the decrease of albedo with time over the grass site was shown in Fig. 1. To see how realistic the snow aging treatment is, we choose the snow periods without new snowfall or snowmelt and without missing data based on the multiyear BOREAS data (from 1994 to 1996). Figure 7 compares the blue-sky albedo from CLM3 and ECMWF with BOREAS data during these periods. For the high snow albedo values over grass, the decay rate of the model albedo is smaller than observed data (Figs. 7a,b). The relatively fast decrease of snow albedo is consistent with previous studies (e.g., Baker et al. 1990). However, for lower snow albedo values over grass, the snow aging effect from the models is close to observation. Over the forest site, the snow albedo is much lower than over the grass site, and the decrease of albedo is slow with time (Figs. 7d–f). Further studies are still needed to address the snow aging process using observational data from longer periods without snowfall or snowmelt.

5. Sensitivity tests to understand the differences between model results and data

Figure 6 provides a robust measure of the performance of each land model. Although model formulations or parameters can be tuned to reduce substantially the albedo bias, excessive tuning usually reduces the transferability of revised formulations or parameters to other regions over global land. Furthermore, there is an inherent difference between point measurements and gridcell average albedos from models. Therefore, based on our understanding of each land model from Figs. 1–7, our goal here is to demonstrate that even minor changes to each model can significantly improve each model's performance. It goes beyond the scope of this study to optimize all relevant parameters and formulations to minimize the model–data difference.

For NG, there is a significant overestimate of albedo over forest (Fig. 6b), whereas the albedo bias is much smaller in magnitude over grass (Fig. 6a). Because NG does not explicitly consider the snow shading effect of trees, our suggestion is to replace the global constant diffuse snow albedo (i.e., 0.9 and 0.75 for the VIS and NIR bands, or 0.825 for the shortwave band) in Eq. (7) by the vegetation-type-dependent maximum snow albedo derived from the bidirectional reflectance distribution function/albedo, reflectance, and land cover measured from the MODIS sensor on board the *Terra* and *Aqua* satellites (Barlage et al. 2005). Because the

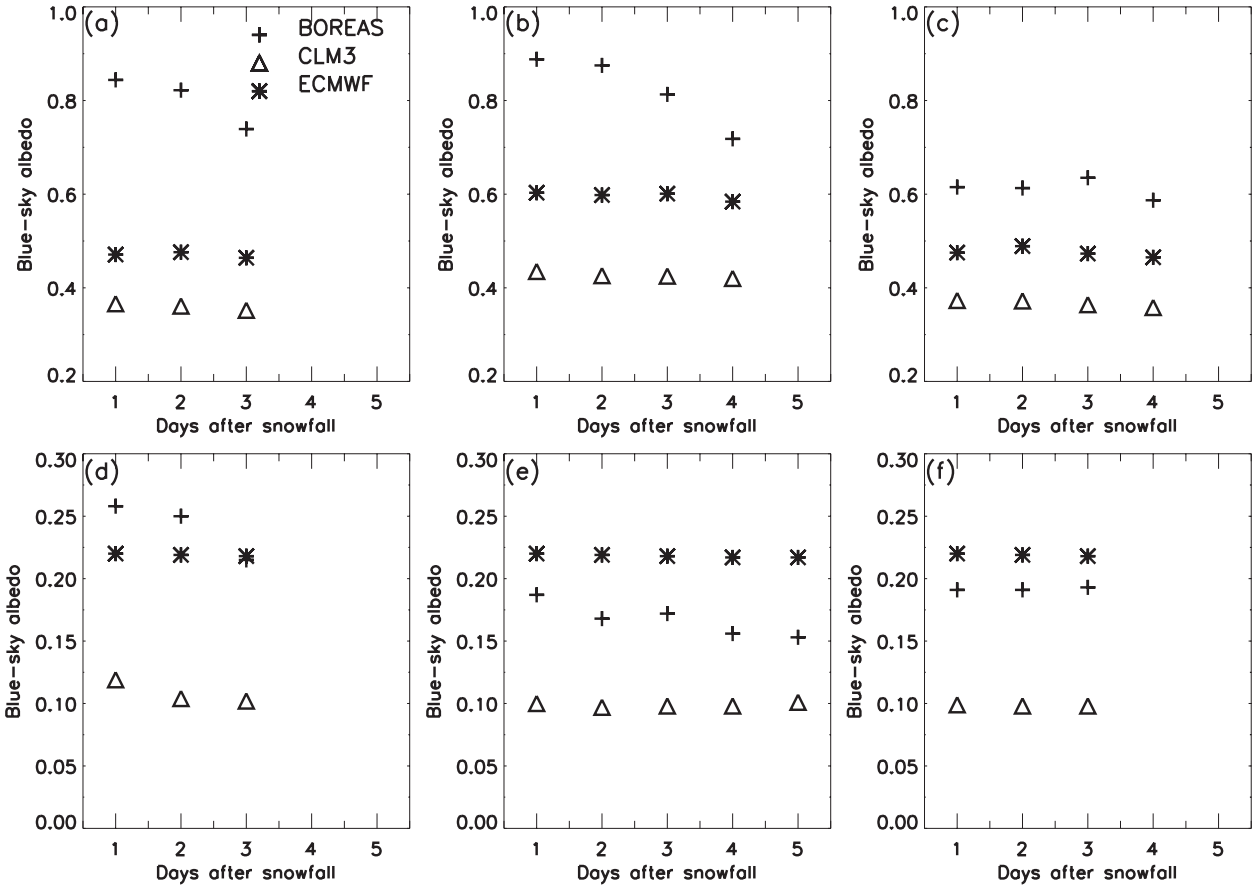

FIG. 7. Comparison of blue-sky albedos from CLM3 and ECMWF with the BOREAS data during the periods without new snowfall or snowmelt over the grass site during (a) 12–14 Nov 1995, (b) 18–21 Jan 1996, and (c) 6–10 Mar 1996 and over the forest site during (d) 22–24 Jan 1995, (e) 5–9 Mar 1995, and (f) 6–8 Mar 1996.

MODIS maximum snow albedo differs most from $(0.9 + 0.75) \times 0.5 = 0.825$ as used in NG over forests, the effect is most significant over forests (rather than over short vegetation), as demonstrated in Fig. 8.

For the Noah land model, W_{cr} is a critical parameter controlling the computation of snow fraction in Eq. (3). Because Noah significantly underestimates albedo over grass (Fig. 6a) but overestimates albedo over forest (Fig. 6b), it is necessary to reduce W_{cr} for short vegetation but increase it for tall vegetation. Therefore, our suggestion is to use $W_{cr} = 0.01$ m for short vegetation and $W_{cr} = 0.2$ m for tall vegetation in Eq. (3) (in contrast to 0.04 and 0.08 m used in Noah, respectively). Furthermore, although satellite-based maximum snow albedo is used over each grid cell in Noah as implemented at NCEP, a specified value for each vegetation type is used for Noah as implemented in the NCAR version of WRF. In our Noah tests so far, the MODIS maximum snow albedos (Barlage et al. 2005) are used. Therefore, we have also done sensitivity tests using the vegetation-type-dependent maximum snow albedo as used in WRF at NCAR. Figure 9 summarizes the sensitivity of Noah to W_{cr} and maximum snow albedo. Over the grass site, the MODIS albedo is similar to the default value used in the NCAR version of WRF, whereas the decrease of W_{cr} from 0.04 to 0.01 m reduces the albedo bias by more than 50% (Fig. 9a). Over the forest site, using the revised W_{cr} value significantly reduces the Noah albedo bias, whereas the use of the maximum snow albedo from WRF at NCAR significantly increase the Noah albedo bias (Fig. 9b). Note that, although the aging effect of snow density is considered, the direct effect of aging on snow albedo is not considered in Noah. For instance, the fresh snow albedo is generally higher than the MODIS value of 0.7 as used in Fig. 9a, and the explicit inclusion of the aging effect on snow albedo (with a higher fresh snow albedo than the MODIS maximum snow albedo) would further reduce the Noah albedo bias in Fig. 9a.

For ECMWF, there is an underestimate of albedo over grass (Fig. 6a), and our suggestion is simply to revise the snow fraction formulation as

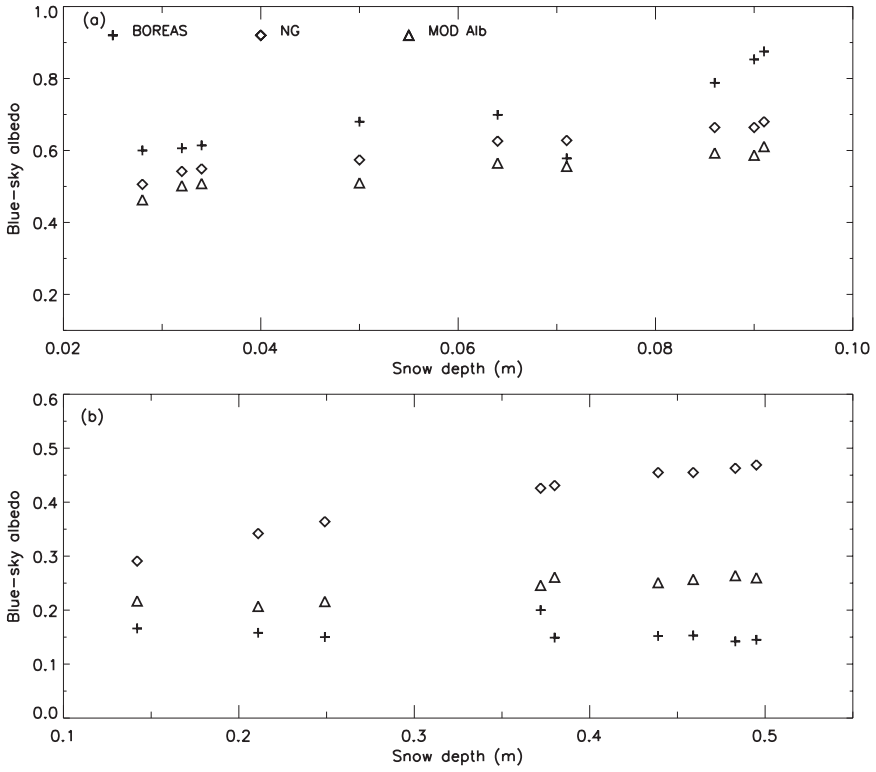

FIG. 8. The sensitivity of NG snow-covered surface albedo to maximum snow albedo over the (a) grass and (b) forest sites using the data in Fig. 6. The MODIS averaged maximum snow albedo values that are dependent on vegetation type (0.70 and 0.34 for grass and evergreen needleleaf forest, respectively) are used in the sensitivity test.

$$c_{\mathrm{sn}} = \min\left[1, \left(\frac{W}{W_{\mathrm{cr}}}\right)^{0.5}\right]. \tag{16}$$

Figure 10 shows that this revision reduces the albedo bias by more than 50% over grass without affecting the already good results over forest.

For CLM3, there is a substantial underestimate of albedo over grass (Fig. 6a), and this is related to the computation of ground snow fraction [i.e., Eq. (8)]. Previous studies (e.g., Niu and Yang 2007) and Fig. 3a have demonstrated the underestimate of snow fraction using Eq. (8). This can be easily understood: because $10z_{0m,g}$ in Eq. (8) roughly represents the height of ground elements, snow as deep as these elements only covers 50% of the ground based on Eq. (8) rather than fully covering the ground. It needs to be emphasized that the use of Eq. (8) in the original BATS land model (Dickinson et al. 1993) is not necessarily as bad because of compensating effects of other BATS components for the computation of snow albedo. For CLM3 in which snow burial fraction and radiative transfer through canopy are computed, Eq. (8) needs to be revised, and our suggestion is simply to drop the factor 10 from the term $10z_{0m,g}$ in Eq. (8):

$$f_{\mathrm{sno}} = \frac{z_{\mathrm{sn}}}{z_{0m,g} + z_{\mathrm{sn}}}. \tag{17}$$

This revision substantially reduces the albedo underestimate over grass (Fig. 11a) without much effect over forest (Fig. 11b).

Because the radiative transfer through canopy is explicitly computed (using the two-stream approximation) in CLM3, an important question is how LAI and SAI affect snow albedos. Zhou et al. (2003) found that, among the variables used to calculate model albedo, LAI and SAI are tightly linked with the spatial pattern and magnitude of the albedo biases, especially over regions with large albedo biases. The vegetation reduces snow albedo through an increase in solar absorption (in particular in the VIS band) by vegetation, a reduction in openings exposed to sun, and an increase in the fraction of shadow. Oleson et al. (2003) demonstrated that a positive model albedo bias may be caused by the underestimate of LAI and SAI, because a sparser canopy would result in more snow-covered ground being

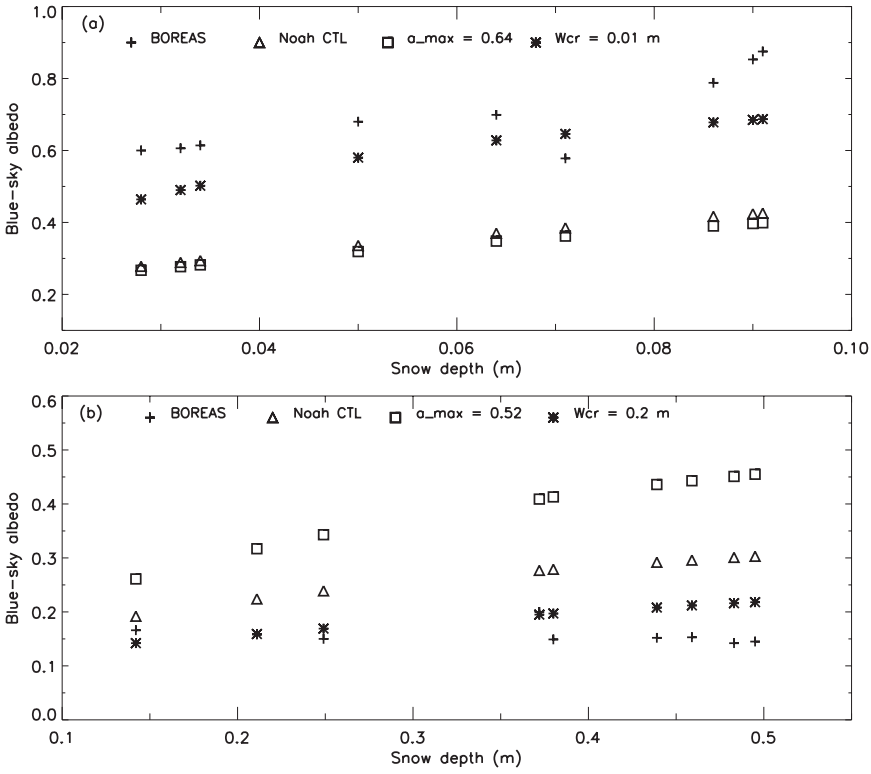

FIG. 9. Sensitivity of Noah snow albedo to the use of maximum snow albedo as used in WRF (at NCAR) and revised W_{cr} values in Eq. (8) over the (a) grass and (b) forest sites using the data in Fig. 6.

exposed. Here we further address the effect of LAI and SAI through sensitivity tests with SAI = 0 or 0.5 and LAI = 0.5, 1, 1.5, and 3 using data in Fig. 6. Over the grass site, LAI and SAI have no effects because of relatively deep snow (0.45 m; Figs. 12a,b). Over the forest site, however, both LAI and SAI affect the mean albedo and the SZA dependence of snow albedo (Figs. 12c,d). In particular, CLM3 results are closest to measurements with LAI + SAI = 1 (i.e., LAI = 1 and SAI = 0 in Fig. 12c and LAI = 0.5 and SAI = 0.5 in Fig. 12d). It is also interesting to note that, while the albedo increases with SZA (i.e., decreases with cosθ) at a relatively high LAI + SAI in Figs. 12c,d, the albedo actually increases with cosθ at a small LAI + SAI (in particular for SAI = 0 and LAI = 0.5 in Fig. 12c). Although the former is usually expected, the latter is correct as well because at local noon (with the highest cosθ) the forest shading effect of underlying snow is small.

6. Conclusions

Although some previous studies have evaluated the snow albedo as part of an overall land model study, it is difficult to conclude whether the snow albedo treatment itself in land models is appropriate. Complementary to the previous studies, we have addressed this issue in this study by directly testing the snow albedo formulations used at some of the major weather forecasting and climate research centers, including the Noah land model used at the NCEP regional and global forecasting models and at the NCAR WRF, the Hou et al. (2002) scheme for albedo computation used for NCEP global forecasting models (denoted here as NG), the NCAR CLM3, and the ECMWF land model.

First, four idealized cases at the BOREAS grass and forest sites were designed to better understand the different albedo formulations in these models. The diffuse albedos from Noah and NG do not change with time because of a constant SWE assumption in the idealized cases. However, the diffuse albedos from CLM3 and ECMWF decrease with time because of the snow aging effect. The SZA dependence of albedo is neglected in Noah and ECMWF, whereas it is considered in NG and CLM3. Over the grass site, ECMWF snow fraction reaches unity first at a snow depth of 15 cm. In contrast, the ground is still not fully covered in CLM3 or NG even with 1 m of snow. Over the forest site, the increase of snow fraction with snow depth is slowest in NG. Although

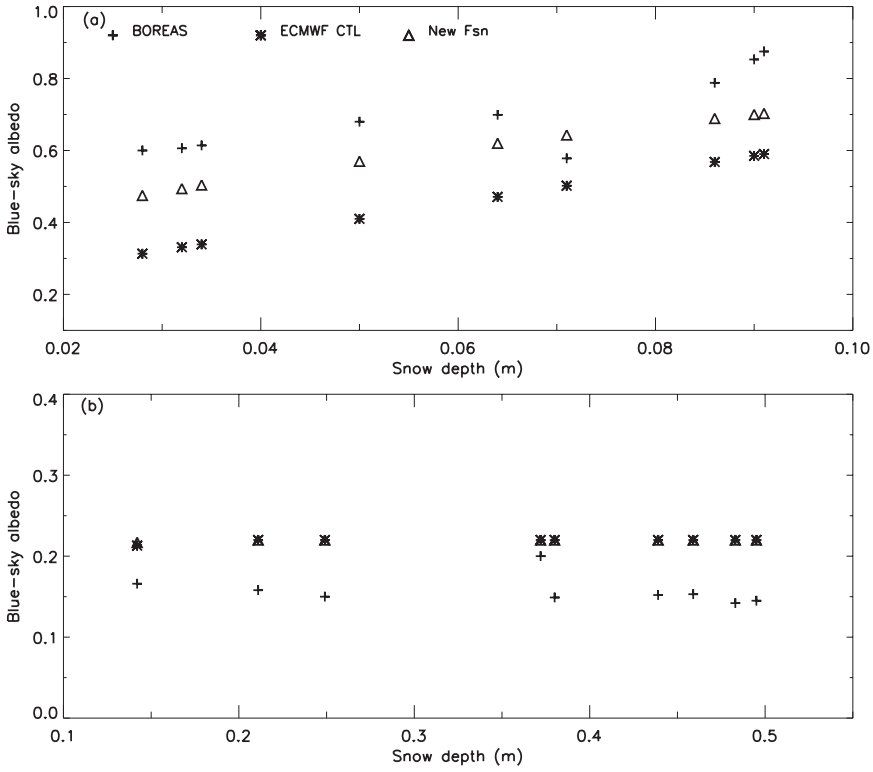

FIG. 10. The sensitivity of ECMWF snow-covered surface albedo to the control [i.e., Eq. (2)] and new [i.e., Eq. (18)] snow fraction formulations over the (a) grass and (b) forest sites using the data in Fig. 6.

the diffuse albedo over the forest site converges to a much smaller value than over the grass site in Noah, ECMWF, and CLM3, it still increases with snow depth in NG even after snow depth is higher than 1 m, which is incorrect.

Then, the BOREAS in situ data were used to evaluate model snow albedo and relevant processes. Because we intend to test model albedo formulations directly (without running the land model), only the periods with snow on the ground but without snowfall or snowmelt were chosen for the comparison. Over the BOREAS grass site, CLM3, Noah, and, to a lesser degree, ECMWF underestimate the blue-sky albedo because of relatively small snow fraction, whereas the NG albedo is closest to observations because of its highest snow fraction among the four models for shallow snow. Over the forest site, ECMWF results are close to observations because a constant albedo for snow under trees is prescribed based on BOREAS observations. CLM3 also provides reasonable results because the two-stream approximation can partially handle the forest shading effect. Noah slightly overestimates snow albedo. Because NG treats snow above grass and snow under trees in the same way, it significantly overestimates snow albedo over the forest site. The decrease of observed albedo with time because of the snow age effect is most significant for high snow albedo values over grass, whereas this decrease is more moderate (in absolute value) when the albedo itself is relatively small (e.g., over the forest site). CLM and ECMWF can reasonably simulate the latter, but they fail to simulate the former.

Based on these analyses, we have come up with ideas that involve only minor changes in parameters or formulations in each model to significantly improve each model's performance. For NG, replacing the globally constant diffuse snow albedo by the vegetation-type-dependent MODIS maximum snow albedo would significantly improve the albedo computation over forest. For Noah, using $W_{cr} = 0.01$ m for short vegetation and $W_{cr} = 0.2$ m for tall vegetation in the snow fraction computation would significantly reduce Noah's underestimate of snow albedo over grass and overestimate over forest. Sensitivity tests also show that using the vegetation-type-dependent maximum snow albedo as used in WRF/Noah at NCAR would significantly increase Noah's albedo bias over forest, suggesting that the MODIS maximum snow albedo data should be used in WRF/Noah. For ECMWF, using the square root of

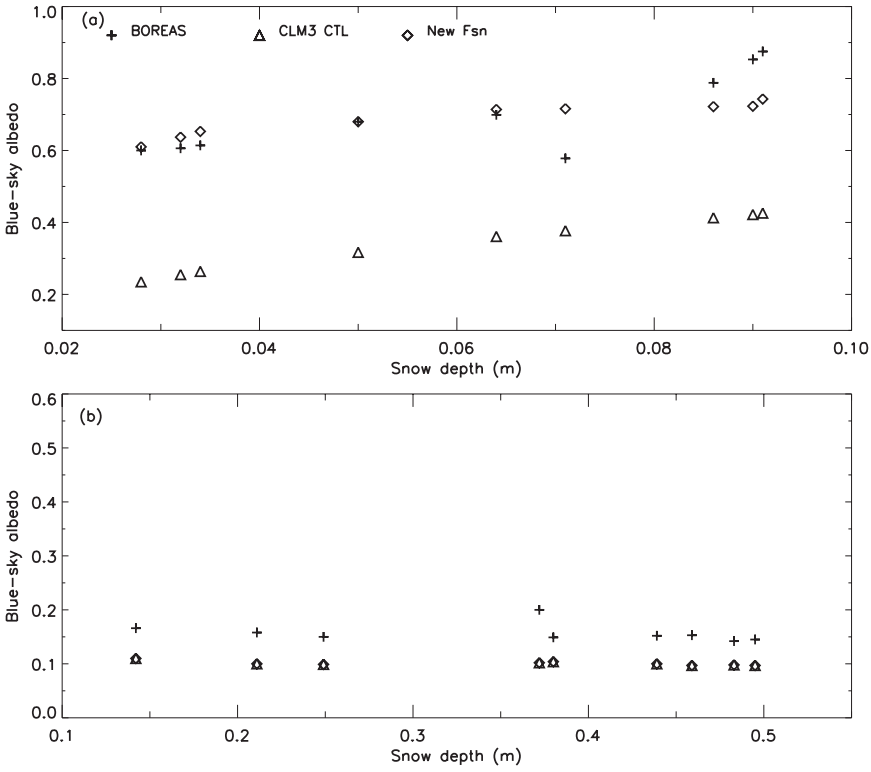

FIG. 11. The sensitivity of CLM3 snow-covered surface albedo to the control [i.e., Eq. (13)] and new [i.e., Eq. (19)] ground snow fraction formulations over the (a) grass and (b) forest sites using the data in Fig. 6.

SWE (rather than SWE itself) in the snow fraction formulation would reduce the albedo bias by more than 50% over grass without affecting the good results over forest. For CLM3, simply dropping the factor 10 from the term $10z_{0m,g}$ in ground snow fraction formulation would substantially reduce the albedo underestimate over grass without much effect over forest. Our sensitivity tests also show that the effect of LAI and SAI is very small over grass in CLM3. However, both LAI and SAI affect the mean albedo and SZA dependence over forest.

Through this study, we have not solved the difficult problem of snow albedo computation; instead, we have made some progress by identifying and understanding model deficiencies and making suggested minor revisions to significantly improve the performance of each of the four land models. These revisions are easy to implement in these models. To assess the robustness of our revisions, we have also used measurements from a grass site in Barrow, Alaska (71.32°N, 156.62°W; see http://www.arm.gov/sites/nsa/C1/), and results are fully consistent with those over the BOREAS grass site (figure not shown): our minor revisions significantly reduce the albedo underestimation by Noah and CLM3 as well as by the ECMWF land model for snow depth less than 0.15 m (i.e., snow fraction less than 1), and their effect on NG is small. In a similar way, we have used measurements over the Hyytiala forest site (61.85°N, 24.28°E) in Finland (Vesala et al. 1998; Hannuniemi et al. 2007), and the results are fully consistent with those over the BOREAS forest site (figure not shown): our minor revisions significantly improve the albedo overestimation in NG and Noah, and their effect on CLM3 and ECMWF is minimal.

Even though we have focused on four specific land models, some of the conclusions are relevant to all land models. For instance, snow fraction cannot be evaluated independently (i.e., without considering the snow albedo formulation). In other words, the same snow fraction could yield very different snow albedos in different models. For this reason, we are not attempting to give a single snow fraction formulation for all land models here. Although the use of satellite maximum snow albedo (e.g., from MODIS) is overall beneficial, additional factors (e.g., the snow aging effect and the possibly higher albedo of fresh snow intercepted by canopy than the MODIS albedo) need to be considered—in particular, over forest regions. Although verification using additional data is needed, our data analyses indicate that the snow

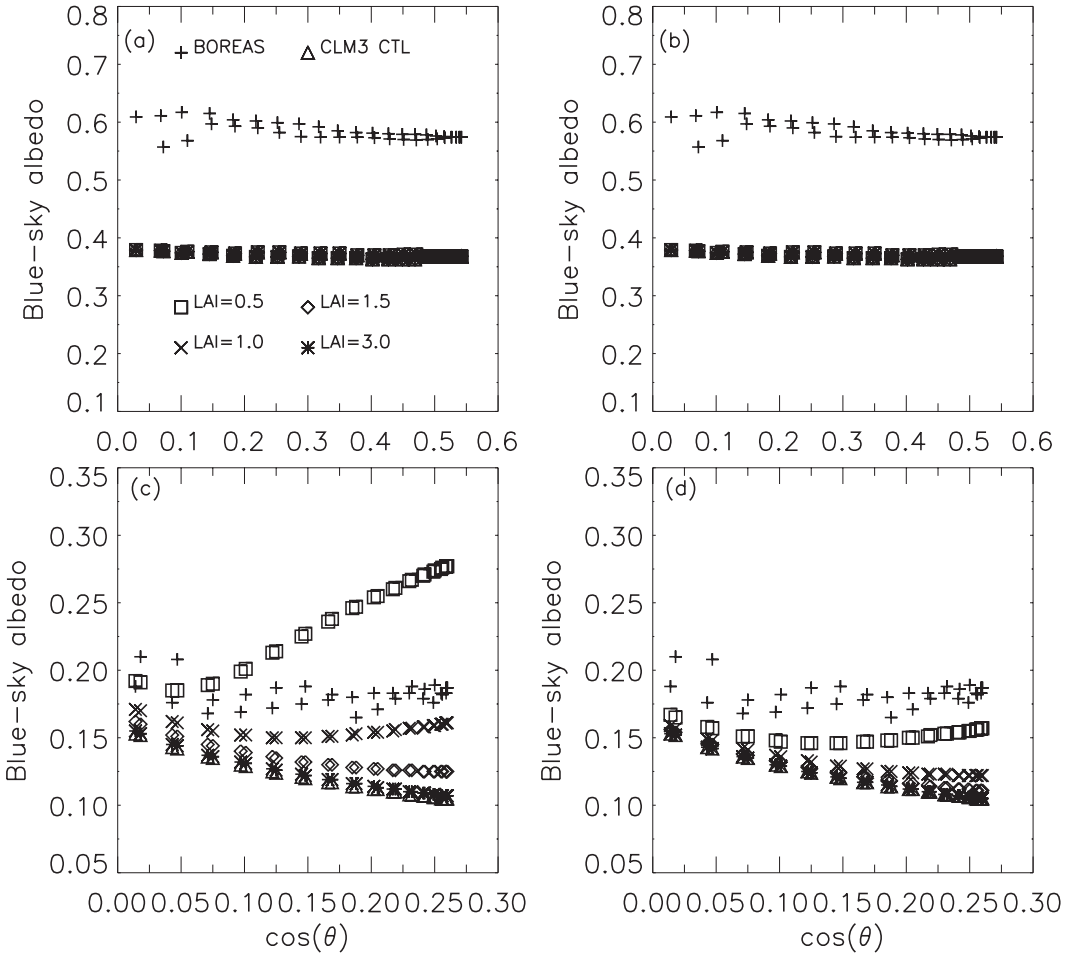

FIG. 12. The sensitivity of CLM3 snow-covered surface albedo to LAI (0.5, 1, 1.5, or 3) and SAI (0, 0.5) over the grass and forest sites using data in Fig. 5: (a) the grass site with SAI = 0, (b) the grass site with SAI = 0.5, (c) the forest site with SAI = 0, and (d) the forest site with SAI = 0.5. Note that all model results overlap in (a) and (b).

albedo decrease with time is most significant when albedo itself is high.

The albedo formulations in NG, ECMWF, and Noah are relatively simple and empirical, but they are inferred from observations. In contrast, the two-stream radiative transfer scheme in CLM3 is more complicated and is based on radiative transfer theory, but it contains several assumptions, as discussed in section 2. In particular, the two-stream scheme in CLM3 does not treat canopy shading effect well. Progress has been made in recent years to address this issue by developing the four-stream scheme (Tian et al. 2007) or by improving the two-stream scheme (Pinty et al. 2006). Even more realistic for the computation of surface albedo and radiative transfer through canopy would be the three-dimensional Monte Carlo models, but the potential use of such models in global weather and climate studies still has a long way to go.

Acknowledgments. This work is supported by NOAA Grant NA07NES4400002 and NASA Grant NNG06GA24G. We thank Drs. Kenneth Mitchell and Yu-Tai Hou for their very useful suggestions to improve the manuscript. Michael Brunke's help in improving the readability of the manuscript is also appreciated. We especially thank three reviewers for detailed and insightful comments, which helped to improve the clarity of our presentation.

REFERENCES

Anderson, E., 1973: National Weather Service River Forecast System: Snow accumulation and ablation model. NOAA Tech. Memo. NWS HYDRO-17, 217 pp.

——, 1976: A point energy and mass balance model of a snow cover. NOAA Tech. Rep. NWS 19, 150 pp.

Baker, D. G., D. L. Ruschy, and D. B. Wall, 1990: The albedo decay of prairie snows. *J. Appl. Meteor.,* **29,** 179–187.

Barlage, M., X. Zeng, H. Wei, and K. E. Mitchell, 2005: A global 0.05° maximum albedo dataset of snow-covered land based on MODIS observations. *Geophys. Res. Lett.,* **32,** L17405, doi:10.1029/2005GL022881.

Betts, A. K., and J. H. Ball, 1997: Albedo over the boreal forest. *J. Geophys. Res.,* **102,** 28 901–28 909.

Bonan, G. B., 1996: A land surface model (LSM version 1.0) for ecological, hydrological, and atmospheric studies: Technical description and user's guide. NCAR Tech. Note NCAR/TN-417+STR, 150 pp.

——, D. Pollard, and S. L. Thompson, 1992: Effects of boreal forest vegetation on global climate. *Nature,* **359,** 716–718.

Boone, A., and P. Etchevers, 2001: An intercomparison of three snow schemes of varying complexity coupled to the same land surface model: Local-scale evaluation at an alpine site. *J. Hydrometeor.,* **2,** 374–394.

Briegleb, B. P., 1992: Delta-Eddington approximation for solar radiation in the NCAR Community Climate Model. *J. Geophys. Res.,* **97,** 7603–7612.

——, P. Minnis, V. Ramanathan, and E. Harrison, 1986: Comparison of regional clear-sky albedos inferred from satellite observations and model computations. *J. Climate Appl. Meteor.,* **25,** 214–226.

Cess, R. D., and Coauthors, 1991: Interpretation of snow–climate feedback as produced by 17 general circulation models. *Science,* **253,** 888–892.

Chen, F., and J. Dudhia, 2001: Coupling an advanced land surface–hydrology model with the Penn State–NCAR MM5 modeling system. Part I: Model implementation and sensitivity. *Mon. Wea. Rev.,* **129,** 569–585.

Dickinson, R. E., 1983: Land surface processes and climate—Surface albedos and energy balance. *Advances in Geophysics,* Vol. 25, Academic Press, 305–353.

——, A. Henderson-Sellers, P. J. Kennedy, and M. F. Wilson, 1986: Biosphere–Atmosphere Transfer Scheme (BATS) for the NCAR Community Climate Model. NCAR Tech. Note NCAR/TN-275+STR, 69 pp.

——, ——, and ——, 1993: Biosphere–Atmosphere Transfer Scheme (BATS) version 1e as coupled to the NCAR Community Climate Model. NCAR Tech. Note NCAR/TN-387+STR, 72 pp.

Douville, H., J. F. Royer, and J. F. Mahfouf, 1995: A new snow parameterization for the Météo-France climate model. *Climate Dyn.,* **12,** 21–35.

Hannuniemi, H., J. Rinne, and T. Manninen, 2007: Snow melting detection in Finland using the CM-SAF weekly surface albedo product (SAL). *Proc. EUMETSAT Meteorological Satellite Conf.,* Amsterdam, Netherlands, EUMETSAT, 7 pp. [Available online at http://www.eumetsat.int/Home/Main/AboutEUMETSAT/Publications/ConferenceandWorkshopProceedings/2007/groups/cps/documents/document/pdf_conf_p50_s4_08_manninen_p.pdf.]

Hou, Y. T., S. Moorthi, and K. Campana, 2002: Parameterization of solar radiation transfer in the NCEP models. NCEP Office Note 441, 46 pp.

Jordan, R., 1991: A one-dimensional temperature model for a snow cover. U.S. Army Cold Regions Research and Engineering Laboratory Special Report 91-16, 49 pp.

Koren, V., J. Schaake, K. Mitchell, Q.-Y. Duan, F. Chen, and J. M. Baker, 1999: A parameterization of snowpack and frozen ground intended for NCEP weather and climate models. *J. Geophys. Res.,* **108,** 19 569–19 585.

Marshall, S. E., and S. G. Warren, 1987: Parameterization of snow albedo for climate models. *Large Scale Effects of Seasonal Snow Cover,* B. E. Goodison, R. G. Barry, and J. Dozier, Eds., IAHS–AIHS Publ. 166, 43–50.

Mitchell, K. E., and Coauthors, 2004: The multi-institution North American Land Data Assimilation System (NLDAS): Utilizing multiple GCIP products and partners in a continental distributed hydrological modeling system. *J. Geophys. Res.,* **109,** D07S90, doi:10.1029/2003JD003823.

Niu, G.-Y., and Z.-L. Yang, 2007: An observation-based formulation of snow cover fraction and its evaluation over large North American river basins. *J. Geophys. Res.,* **112,** D21101, doi:10.1029/2007JD008674.

Oleson, K. W., G. B. Bonan, C. Schaaf, F. Gao, Y. Jin, and A. Strahler, 2003: Assessment of global climate model land surface albedo using MODIS data. *Geophys. Res. Lett.,* **30,** 1443, doi:10.1029/2002GL016749.

——, and Coauthors, 2004: Technical description of the community land model (CLM). NCAR Tech. Note NCAR/TN-461+STR, 173 pp.

Pinty, B., T. Lavergne, R. E. Dickinson, J. L. Widlowski, N. Gobron, and M. M. Verstraete, 2006: Simplifying the interaction of land surface with radiation for relating remote sensing products to climate models. *J. Geophys. Res.,* **111,** D02116, doi:10.1029/2005JD005952.

Qu, X., and A. Hall, 2006: Assessing snow albedo feedback in simulated climate change. *J. Climate,* **19,** 2617–2630.

Robinson, D. A., and G. Kukla, 1985: Maximum surface albedo of seasonally snow-covered lands in the Northern Hemisphere. *J. Climate Appl. Meteor.,* **24,** 402–411.

Sellers, P. J., 1985: Canopy reflectance, photosynthesis and transpiration. *Int. J. Remote Sens.,* **6,** 1335–1372.

——, and Coauthors, 1995: The Boreal Ecosystem–Atmosphere Study (BOREAS): An overview and early results from the 1994 field year. *Bull. Amer. Meteor. Soc.,* **76,** 1549–1577.

——, and Coauthors, 1997: BOREAS in 1997: Experiment overview, scientific results, and future directions. *J. Geophys. Res.,* **102,** 28 731–28 769.

Shewchuk, S. R., 1997: Surface mesonet for BOREAS. *J. Geophys. Res.,* **102,** 29 077–29 082.

Slater, A. G., and Coauthors, 2001: The representation of snow in land surface schemes: Results from PILPS 2(d). *J. Hydrometeor.,* **2,** 7–25.

Tian, Y., R. E. Dickinson, L. Zhou, R. B. Myneni, M. Friedl, C. B. Schaaf, M. Carroll, and F. Gao, 2004: Land boundary conditions from MODIS data and consequences for the albedo of a climate model. *Geophys. Res. Lett.,* **31,** L05504, doi:10.1029/2003GL019104.

——, ——, and ——, 2007: Four-stream isosector approximation for canopy radiative transfer. *J. Geophys. Res.,* **112,** D04107, doi:10.1029/2006JD007545.

Vesala, T. J., and Coauthors, 1998: Long-term field measurements of atmosphere–surface interactions in boreal forest ecology, micrometeorology, aerosol physics and atmospheric chemistry. *Trends Heat Mass Momentum Transfer,* **4,** 17–35.

Viterbo, P., and A. K. Betts, 1999: Impact on ECMWF forecasts of changes to the albedo of the boreal forests in the presence of snow. *J. Geophys. Res.,* **104,** 27 803–27 810.

Wang, Z., and X. Zeng, 2008: Snow albedo's dependence on solar zenith angle from in situ and MODIS data. *Atmos. Oceanic Sci. Lett.,* **1,** 45–50.

——, ——, M. Barlage, R. E. Dickinson, F. Gao, and C. B. Schaaf, 2004: Using MODIS BRDF and albedo data to evaluate global model land surface albedo. *J. Hydrometeor.,* **5,** 3–14.

Warren, S. G., 1982: Optical properties of snow. *Rev. Geophys. Space Phys.,* **20,** 67–89.

——, and W. J. Wiscombe, 1980: A model for the spectral albedo of snow. II: Snow containing atmospheric aerosols. *J. Atmos. Sci.,* **37,** 2724–2745.

Wiscombe, W. J., and S. G. Warren, 1980: A model for the spectral albedo of snow. I: Pure snow. *J. Atmos. Sci.,* **37,** 2712–2733.

Yang, Z. L., R. E. Dickinson, A. Robock, and K. Y. Vinnikov, 1997: Validation of the snow submodel of the biosphere–atmosphere transfer scheme with Russian snow cover and meteorological observational data. *J. Climate,* **10,** 353–373.

Zhou, L., and Coauthors, 2003: Comparison of seasonal and spatial variations of albedos from Moderate-Resolution Imaging Spectroradiometer (MODIS) and Common Land Model. *J. Geophys. Res.,* **108,** 4488, doi:10.1029/2002JD003326.